6056 ALLOY: STUDY OF THE CORROSION BEHAVIOUR OF COARSE INTERMETALLIC PARTICLES IN CHLORIDE AND SULPHATE MEDIA THROUGH PHASE SHIFTING INTERFEROMETRIC MICROSCOPY OBSERVATIONS

Valérie GUILLAUMIN, Christine BLANC, Yves ROQUES and Georges MANKOWSKI

Laboratoire de Cristallochimie, Réactivité et Protection des Matériaux,
UPRESA CNRS 5071, ENSCT, 118 route de Narbonne, 31077 Toulouse Cedex 04, France

ABSTRACT The corrosion behaviour of the two types of coarse intermetallic particle present in the 6056 T6 alloy was studied in chloride and sulphate solutions by phase shifting interferometric microscopy. The influence of overageing was also determined. The two types of particle did not present the same behaviour: the Mg-Si-rich particles dissolved during polarization in chloride or sulphate solutions whereas the Si-Mn-Fe-rich particles led to the dissolution of the surrounding matrix. But, this behaviour depended on the time of overageing.

Keywords: *aluminium, intermetallics, corrosion, overageing, interferometric microscopy.*

1. INTRODUCTION

The 6056 T6 aluminium alloy, which has recently been developed to replace the 2024 T3 alloy in aircraft structures, seems to be susceptible to different forms of corrosion, such as intergranular and pitting corrosion. But, very few works have studied the corrosion properties of this alloy. Phase shifting interferometric microscopy (PSIM) was used to study the behaviour of the intermetallic particles present in the 6056 T6 alloy after immersion or polarization in water, sulphate and chloride solutions. The influence of overageing was also determined by PSIM. This technique provides sufficient lateral resolution considering the dimensions of the intermetallic particles and a very high resolution in depth.

2. EXPERIMENTAL SET UP

PSIM [1] is based on classical interferometry (Fig. 1). A light beam emerging from a visible light source (wavelength λ) is split into two beams. One is reflected by a reference mirror and the other by the sample surface. After reflexion, the two beams are recombined so they generate an interference pattern giving an image of the sample point by point. The advantage of PSIM consists of the acquisition of four images of the same surface. Each image is recorded with a CCD camera and stored on a hard disk. A difference of $\lambda/4$ in optical path length between two consecutive images is obtained by varying the distance between the sample and the interferometric objective. The position of the reference mirror is controlled by activating piezoelectric transducers. The treatment consists in determining the height of each point z(x,y) of the image knowing the four intensities $I_1(x,y)$, $I_2(x,y)$, $I_3(x,y)$ and $I_4(x,y)$ at differences of optical path length 0, $\lambda/4$, $\lambda/2$, $3\lambda/4$. The surface profile is given by:

$$z(x,y) = (\lambda/4\pi) \arctan [I_4(x,y) - I_2(x,y)]/[I_1(x,y) - I_3(x,y)] \quad (1)$$

The experimental apparatus consisted in a metallurgical microscope with a Mireau interferometric objective (Optiphot, Nikon) associated with a CCD camera (512x512 pixels), an

analog-to-digital image conversion card and a personal computer. Digital conversion was made 2^8 levels. This led to a vertical resolution of $\lambda/(2x256)$. With the light used (λ = 577 nm) corresponded to approximately 1 nm. The lateral resolution was that of a conventional objective our case a x40 objective was chosen leading to a lateral resolution of 0.4 μm.

The software allowed roughness determination, correction of tilt angle and determination of and 3D profiles. Comparison of corroded and non-corroded surfaces was very easy. Accurate repositioning of the sample was possible: 3D profiles of the same particle were plotted before after corrosion tests. So, any slight attack of intermetallic particles or of areas near them could quantitatively measured.

3. MATERIALS AND EXPERIMENTAL CONDITIONS

The material used was a 3.2 mm thick sheet of 6056 T6 alloy. The T6 state consists of solution heat treatment at 550°C, air quenching and tempering at 175°C for 8 hours. In order to understand the influence of overageing on the behaviour of the material, this alloy was further heat treated at temperature higher than 175°C for different times t_I, t_{II} and t where $t_I<t_{II}<t$; the corresponding samples were referred to as T78-I, T78-II and T78. Table I gives the composition of the material.

Different types of precipitate can be distinguished in the 6056 T6 alloy: hardening precipitates, little precipitates at the grain boundaries or within the grain and coarse intermetallic particles. Two types of coarse intermetallic particle were distinguished in the 6056 T6 alloy: Mg-Si particles (type a) and Si-Mn-Fe-rich particles (type b). The composition of the two types of particle is given in Table II. Figure 2 shows a Scanning Electron Microscopy (SEM) micrograph of the 6056 T6 alloy on which the two types of particle can be observed. In the 6056 T78-I, II and T78 alloy the same two types of coarse intermetallic particle were found.

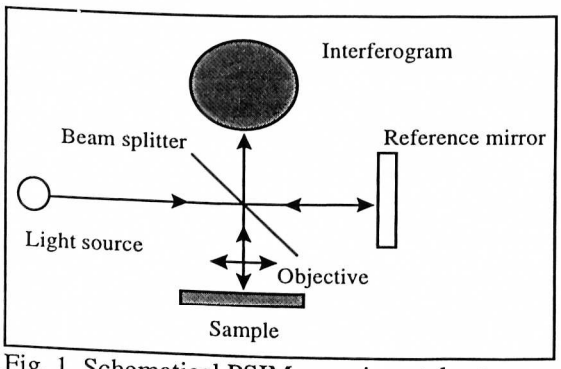

Fig. 1. Schematical PSIM experimental set up

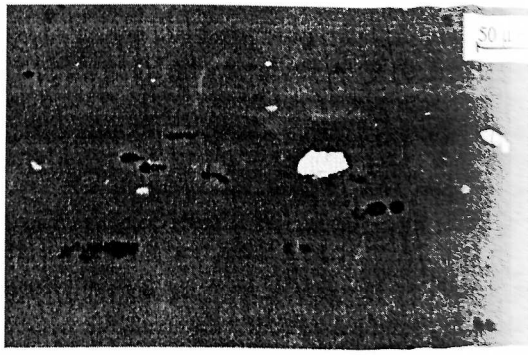

Fig. 2. Coarse intermetallic particles in the 6056 T6 alloy. SEM micrograph

Table I: Composition of the 6056 alloy (wt%)

Al	Si	Cu	Mg	Mn	Fe	Cr	Zn	Ti	Zr
base	0.92	0.87	0.86	0.55	0.19	0.004	0.15	0.02	0.1

Before testing, the samples were mechanically polished from 1000 to 4000 grit SiC paper then with 1 μm diamond paste. The polished samples were observed by PSIM before the corrosion tests: some coarse intermetallic particles were identified and their 2D and 3D profiles plotted. The the samples were immersed in water or polarized at different potentials in 1M NaCl solution or 0.1M Na_2SO_4 solution for different times. The identified particles were located once more and

new profiles plotted and compared to those obtained before immersion in the electrolyte. All potentials quoted are relative to the saturated calomel electrode.

Table II: Composition of coarse intermetallic particles in 6056 T6 alloy (wt%)

	Al	Si	Cu	Mg	Mn	Fe
Type a	base	17.82	0.30	26.40	0.33	0.00
Type b	base	7.35	1.12	0.12	17.64	10.90

4. RESULTS AND DISCUSSION

4.1 Reactivity of coarse intermetallic particles present in the 6056 T6 alloy in different media

3D profiles were plotted for the two types of particle present in the 6056 T6 alloy before and after immersion in water or polarization in chloride or sulphate solutions. On these profiles (Fig. 3), the z axis is very expanded compared to the x and y axes. So, even if the particles appear to have a high relief on the profile, in fact, the mean height of the particles is only equal to a few hundred nanometers. The relief observed after polishing may result from the mechanical polishing (the particles and the matrix not having the same hardness) and also from the particle reactivity towards the lubricant, i.e. water, used during polishing. Indeed, the comparison of the 3D profiles plotted for the same particle after polishing and after five minutes' immersion in water showed that the Mg-Si-rich particles dissolved slightly. On the contrary, Si-Mn-Fe-rich particles did not react in water. The same result was found when the samples were polarized in chloride or sulphate solutions. For example, figure 3 shows that Mg-Si-rich particles are dissolved a little after one hour's polarization in 0.1M Na_2SO_4 solution at 300mV whereas Si-Mn-Fe-rich particles did not react at all.

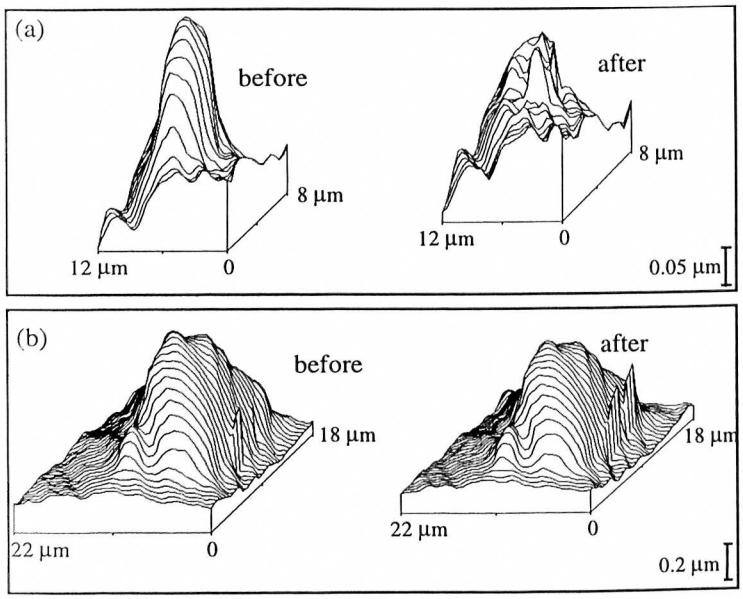

Fig. 3. 3D profiles of (a) a Mg-Si-rich particle and (b) a Si-Mn-Fe-rich particle before and after one hour's polarization in 0.1M Na_2SO_4 at 300mV/SCE.

It was technically difficult to superimpose the 3D profiles plotted before and after immersion in the electrolyte whereas it was easier to make 2D profiles coincide using the non-attacked matrix level as a reference. So, in order to quantify the dissolution of Mg-Si-rich particles, 2D profiles were plotted. 2D profiles correspond to sections in a plane perpendicular to the sample surface. They were plotted every 0.4µm for a particle just after polishing. They were plotted again after immersion or polarization in the electrolyte and compared to the previous profiles. Only the 2D

profile of the maximum attack was considered for the quantitative measurement. Figure represents the 2D profiles plotted for a Mg-Si-rich particle before and after one hour's polarization in 0.1M Na_2SO_4 at 300mV. In order to estimate the amount of material lost, the surface between the particle 2D profiles and the matrix level, i.e. S_R before polarization and S_A polarization, were measured. This allowed the surface area lost S_L to be calculated. Since particle sizes varied over a wide range, a parameter R was defined as follows:

$$R = S_L/d_R \qquad (2)$$

R takes into account the size of the particles in the attack plane by including the notion which was the dimension of the particle measured in the 2D profile plotted before immersion. Parameter R then allowed better comparisons to be made between the lost material for particles different sizes. R corresponded to a mean attack depth and was expressed in µm.

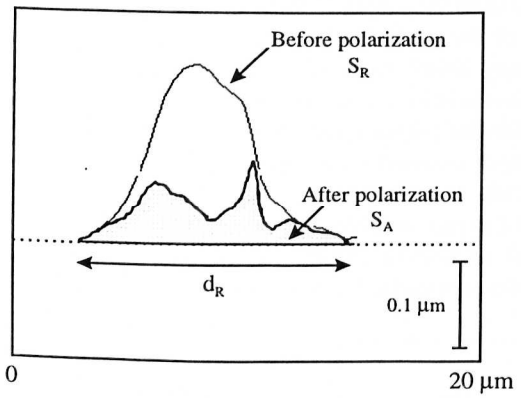

Fig. 4. 2D profiles plotted for a Mg-Si-rich particle present in the 6056 T6 alloy before and after polarization in 0.1M Na_2SO_4 at 300mV/SCE.

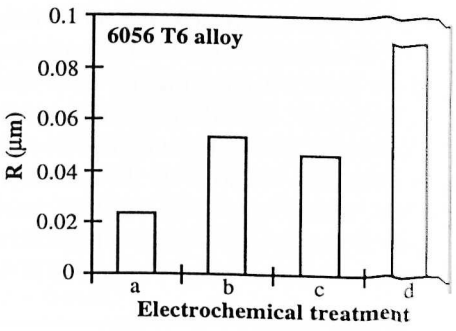

Fig. 5. R values calculated after (a) five minutes' immersion in distilled water (b) and (c) five minutes' polarization in 1M NaCl at -900 mV/SCE and -750 mV/SCE respectively (d) one hour's polarization in 0.1M Na_2SO_4 at 300mV/SCE.

Figure 5 shows a comparison of the R values obtained for the 6056 T6 alloy after different electrochemical treatments. After five minutes' immersion in distilled water, Mg-Si-rich particles dissolved slightly. A five minutes' polarization in 1M NaCl solution at a potential of -750mV or -900mV induced a stronger dissolution of Mg-Si-rich particles compared to the result obtained in water, but the results were the same for the two different potentials, i.e. -900 and -750mV. On the contrary, when the potential became higher than -720mV, which corresponded to the corrosion potential of the 6056 T6 alloy in 1M NaCl, the dissolution of Mg-Si-rich particles strongly increased and it was not possible to calculate the R value anylonger. Sulphate ions appeared to be less agressive towards Mg-Si-rich particles. Indeed, after one hour' s polarization in 0.1M Na_2SO_4 at -300mV/SCE, the dissolution of Mg-Si-rich particles was not significant compared to the slight dissolution of the matrix which did not allow R values to be calculated. However, the dissolution did become significant after one hour' s polarization at higher potentials which appear in figure 5.

4.2 Influence of overageing on the reactivity of coarse intermetallic particles

PSIM analysis was also performed on the 6056 T78-I, T78-II and T78 alloys in order to study the influence of overageing on the reactivity of coarse intermetallic particles. The samples were polarized for an hour in 0.1M Na_2SO_4 at +300mV/SCE. Comparison of 3D and 2D profiles showed that the dissolution of Mg-Si-rich particles was greater for the overaged alloys than for the 6056 T6 alloy. Indeed, for the 6056 T6 alloy, Mg-Si-rich particles were dissolved a little but still appeared as relief on the surface. But, for the overaged alloys, Mg-Si-rich particles were so dissolved that they appeared as a hole in the sample surface. Figure 6 shows the R values obtained for the different heat treatments. The dissolution was very low for the 6056 T6 alloy. But, for the 6056 T78-II and T78 alloys, Mg-Si-rich particles dissolved to a great extent and, for the 6056 T78-I alloy, Mg-Si-rich particle dissolution was so strong that it was not possible to use PSIM.

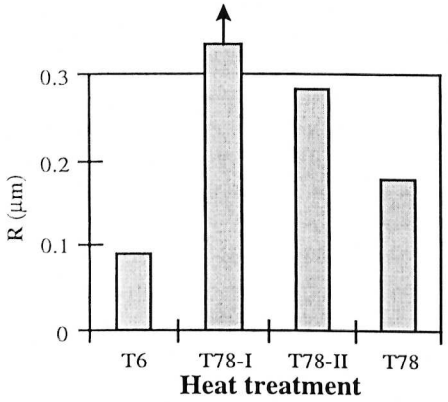

Fig. 6. R versus heat treatment

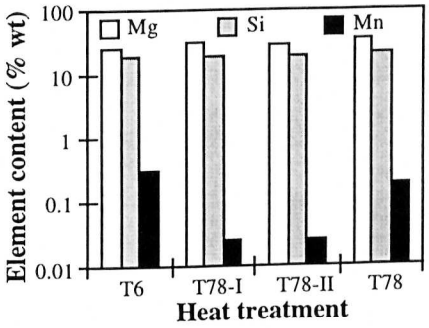

Fig. 7. Mg-Si-rich particle composition versus heat treatment

In order to explain these differences, the particle composition was determined using Energy Dispersed Spectroscopy (EDS) analyses for the different heat treatments (Fig.7). It was found that the only element that differed between heat treatments was manganese. The particles containing more Mn dissolved less than the others. Now, different authors have shown that the addition of manganese to aluminium alloys has little or no effect on corrosion. Manganese tends to combine with aluminium, iron or silicon to form Al_6Mn, (Fe, Mn)Al_6 or (Fe, Mn)$_3Si_2Al_{15}$ which have a corrosion potential similar to that of aluminium [3, 4]. Our results suggest that the presence of Mn in the Mg-Si-rich particles seemed to be advantageous but further results will be necessary to really explain the difference of behaviour between the heat treatments.

The comparison of 3D and 2D profiles plotted before and after polarization in sulphate solution for Si-Mn-Fe-rich particles showed that the same result as for the 6056 T6 alloy was found for the 6056 T78-II and T78 alloys: these particles did not react. On the contrary, for the 6056 T78-I alloy, the matrix surrounding Si-Mn-Fe-rich particles was found to dissolve strongly (Fig. 8).

Therefore, Si-Mn-Fe-rich particles acted as local cathodes towards the matrix in the 6056 T78-I alloy promoting dissolution of the surrounding matrix. The comparison of 2D profiles plotted before and after polarization allowed the dissolution of the surrounding matrix to be quantified. This was performed for several Si-Mn-Fe-rich particles over their whole surface every 0.4µm. It was found that the dissolution was very homogeneous with an average value of 0.03µm with a standard deviation of 0.01µm.

In order to explain the differences between the heat treatments, EDS analyses were performed to determine the composition of Si-Mn-Fe-rich particles, and that of the corresponding surrounding matrix, versus overageing time. For the particle composition, the main difference was the Mg content which was very low in the 6056 T6 alloy but increased with overageing to become equal to 3% for all the overaged alloys. The presence of Mg in the particles in the 6056 T78-I alloy could explain the matrix dissolution as shown by Elboujdaini et al. [5, 6]. For the 6056 T78-II and T78 alloys, the Mg content was the same but no matrix dissolution occurred. For these two alloys, the heat treatment was longer; the alloying elements had longer to diffuse. So, the matrix surrounding the particles in the T78-II and T78 alloys could have a composition different from that in the T78-I alloy which could in turn explain that no matrix dissolution was promoted in the T78-II and T78 alloys. But, EDS analyses were performed and no composition difference of the surrounding matrix in the different alloys was found. Perhaps this analytical technique was not accurate enough to allow such a difference to be shown. So, the change in behaviour from one heat treatment to another could be explained by a variation in the composition of the surrounding matrix but, as yet, no experimental results have allowed this hypothesis to be confirmed.

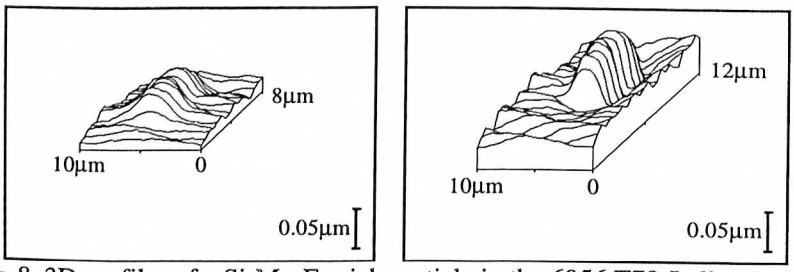

Fig. 8. 3D profiles of a Si-Mn-Fe-rich particle in the 6056 T78-I alloy before and after one hour' s polarization in 0.1M Na_2SO_4 at +300mV/SCE.

5. CONCLUSIONS

This work showed that PSIM is an interesting technique to study the corrosion behaviour of materials, for example the reactivity of intermetallic particles. For the 6056 alloy, the behaviour of the two types of particle seemed to depend on the relative contents of Mg and Mn; the influence of overageing could also be significant.

Acknowledgements - This work was carried out in the framework of the "Laboratoire Régional pour l'Amélioration des Matériaux Structuraux pour l'Aéronautique" with the financial support of the Région Midi-Pyrénées. Special recognition goes to Michelle Reversat for the SEM work.

REFERENCES

[1] R. Escalona, R. Devillers, G. Tribillon, J. Calatroni, P. Fievet, Y. Roques and F. Dabosi: J. Mater. Sci., 28 (1993), 999.
[2] C. Blanc and G. Mankowski: Corros. Sci., 39 (1997), 949.
[3] Aluminium, Properties, Physical Metallurgy and Phase Diagrams: K. R. Van Horn ed., ASM, Metals Park, OH, 1(1971), 212.
[4] P. M. Aziz and H. P. Godard: Ind. Eng. Chem., 44 (1952), 1791.
[5] M. Elboujdaini and E. Ghali: Corros. Sci., 30 (1990), 855.
[6] M. Elboujdaini, E. Ghali, R. G. Barradas and M. Girgis: J. of Appl. Electrochem., 25 (1995), 412.